RESEARCH ARTICLE

Assessment of SRM, MRM³, and DIA for the targeted analysis of phosphorylation dynamics in non-small cell lung cancer

Thierry Schmidlin[1], Luc Garrigues[1], Catherine S. Lane[2], T. Celine Mulder[1], Sander van Doorn[1], Harm Post[1], Erik L. de Graaf[1,3], Simone Lemeer[1], Albert J. R. Heck[1] and A. F. Maarten Altelaar[1]

[1] Biomolecular Mass Spectrometry and Proteomics, Bijvoet Center for Biomolecular Research and Utrecht Institute for Pharmaceutical Sciences, Utrecht University and Netherlands Proteomics Centre, Utrecht, The Netherlands
[2] SCIEX, Phoenix House, Lakeside Drive, Centre Park, Warrington, UK
[3] Current address: Erik L. de Graaf, Fondazione Pisana per la Scienza ONLUS, Via Panfilo Castaldi 2, 56121, Pisa, Italy

Hypothesis-driven MS-based targeted proteomics has gained great popularity in a relatively short timespan. Next to the widely established selected reaction monitoring (SRM) workflow, data-independent acquisition (DIA), also referred to as sequential window acquisition of all theoretical spectra (SWATH) was introduced as a high-throughput targeted proteomics method. DIA facilitates increased proteome coverage, however, does not yet reach the sensitivity obtained with SRM. Therefore, a well-informed method selection is crucial for designing a successful targeted proteomics experiment. This is especially the case when targeting less conventional peptides such as those that contain PTMs, as these peptides do not always adhere to the optimal fragmentation considerations for targeted assays. Here, we provide insight into the performance of DIA, SRM, and MRM cubed (MRM³) in the analysis of phosphorylation dynamics throughout the phosphoinositide 3-kinase mechanistic target of rapamycin (PI3K-mTOR) and mitogen-activated protein kinase (MAPK) signaling network. We observe indeed that DIA is less sensitive when compared to SRM, however demonstrates increased flexibility, by postanalysis selection of alternative phosphopeptide precursors. Additionally, we demonstrate the added benefit of MRM³, allowing the quantification of two poorly accessible phosphosites. In total, targeted proteomics enabled the quantification of 42 PI3K-mTOR and MAPK phosphosites, gaining a so far unachieved in-depth view mTOR signaling events linked to tyrosine kinase inhibitor resistance in non-small cell lung cancer.

📖 Additional supporting information may be found in the online version of this article at the publisher's web-site

1 Introduction

Protein phosphorylation is closely linked to multiple cellular processes such as enzyme activation or inhibition,

Correspondence: Dr. A. F. Maarten Altelaar, Biomolecular Mass Spectrometry and Proteomics, Bijvoet Center for Biomolecular Research and Utrecht Institute for Pharmaceutical Sciences, Utrecht University and Netherlands Proteomics Centre, Padualaan 8, 3584 CH Utrecht, The Netherlands
E-mail: m.altelaar@uu.nl

Abbreviations: DDA, data-dependent acquisition; **DIA**, data-independent acquisition; **EGFR**, epidermal growth factor receptor; **HpH**, high-pH; **HR-MRM**, high resolution MRM; **MAPK**, mitogen-activated protein kinase; **MRM³**, MRM cubed; **mTOR**, mechanistic target of rapamycin; **NSCLC**, non-small cell lung cancer; **PRM**, parallel reaction monitoring; **PI3K**, phosphoinositide 3-kinase; **TKI**, tyrosine kinase inhibitor

Significance of the study

The three MS-based targeted proteomics methods SRM, MRM[3], and DIA differ in key parameters such as sensitivity, selectivity, and multiplexing capabilities. By investigating 48 phosphorylation events related to mTOR-PI3K/MAPK signaling, using these three acquisition types, we provide insights into their performance characteristics. mTOR-PI3K/MAPK signaling has been linked to numerous bio-logical processes such as cancer, aging, and neuronal development, making it one of the most investigated biological pathways. With this study we provide crucial information for well-informed method selection, facilitating successful targeted proteomics analysis of the mTOR-PI3K/MAPK signaling pathway as well as protein phosphorylation in general.

protein–protein interaction, cell–cell signaling events, and protein degradation. MS has advanced to be the method of choice to study temporal dynamics of protein phosphorylation events at a proteome wide scale [1, 2].

The majority of MS-based phosphoproteomic research entails a relatively unbiased approach by combing phosphopeptide enrichment protocols with shotgun proteomics as reviewed extensively [3–6]. This enables the identification and quantification of phosphorylation events without any prior knowledge and usually achieves a substantially broad phosphoproteome coverage [7–9], although it introduces a bias toward high abundant phosphopeptides [10]. An alternative is the use of MS-based targeted proteomics, which can circumvent this bias and allows for a more hypothesis-driven approach [11]. Conventionally, MS-based targeted proteomics is performed on triple quadrupole mass spectrometers operated in SRM mode [12]. More recently, analogous methods were developed using high resolution instruments such as the Q Exactive (parallel reaction monitoring, PRM) [13–15] or the TripleTOF (HR-MRM, high resolution MRM) [16]. While SRM applies filters for both, precursor and fragment ions, PRM and HR-MRM rely solely on precursor ion isolation in combination with acquisition of high resolution/accurate mass MS/MS spectra. These full-scan fragment spectra are then used to extract traces of specific fragment ions and their chromatographic peak areas are used for quantification [17].

While SRM is generally regarded as the most sensitive and quantitatively most accurate MS-based method [18], it has drawbacks in terms of a comparably low resolution in both precursor and fragment m/z filtering. This lower resolution may cause interferences to occur, leading to potentially falsified quantitative readouts by integrating peak groups that do not originate from the peptide of interest. PRM and HR-MRM can reduce such effects by acquiring high resolution MS/MS. Another way to overcome this issue is by using a technique called MRM cubed (MRM[3]), implemented on QTRAP instruments. Here, the third quadrupole is replaced by a linear ion-trap, enabling an existing SRM assay to be further refined by isolation and fragmentation of primary fragment ions. This enables monitoring of chromatographic traces originating from secondary fragment ions. While mainly used to increase the specificity of SRM assays so far [19–21], it has also been shown to increase the sensitivity of the assay [22–25].

Another more recent approach in MS-based targeted proteomics is referred to as data-independent acquisition (DIA) or sequential window acquisition of all theoretical spectra [26]. Compared to SRM the acquisition method itself is not targeted per se, but repeatedly cycles through broad consecutive isolation windows, thus fragmenting the whole MS1 range within the chromatographic time scale [27]. Based on prior information obtained from spectral libraries, peak groups for each peptide of interest can be extracted from the highly multiplexed DIA data and quantified by using the sum of the integrated chromatographic fragment peak areas, similar to SRM. As data acquisition in DIA provides continuous fragment ion intensity information across time, it outperforms SRM in multiplexing capability, thus competing with shotgun proteomics in terms of proteome coverage. Moreover, DIA outperforms SRM in ease of use, as no time consuming method development for each peptide of interest is required [28]. However, it does not achieve the sensitivity of an optimized SRM assay yet [27].

So far MS-based targeted proteomics methods were mainly used to obtain quantitative information on protein expression level, with only limited studies focusing on quantifying specific protein PTMs. However, large-scale phosphoproteomics studies often lack the ability to comprehensively map known functional phosphosites throughout selected signaling cascades of interest. Therefore, MS-based targeted phosphoproteomics potentially presents a valuable alternative in the analysis of cellular signaling. An initial study using SRM to quantify phosphopeptides was presented by Unwin et al. in 2005 [29] followed by a handful of studies adopting the phospho-SRM technology to measure different target phosphopeptides (e.g. [30–33]). Approaches to quantify phosphorylation sites by targeted data extraction from DIA analyses are also starting to appear [34, 35]. MRM[3] has so far not been used for phosphopeptide quantification, however, MS3 has shown to be beneficial for targeted phosphopeptide analysis in a pseudo-SRM approach, increasing the dynamic quantification range [25].

Here, we evaluated in parallel SRM, DIA, and MRM[3] for the analysis of phosphorylation dynamics across selected nodes of the phosphoinositide 3-kinase mechanistic target of rapamycin (PI3K-mTOR)/mitogen-activated protein kinase (MAPK) signaling pathway. Involved in a variety of vital

cellular processes such as cell proliferation, cell growth, and survival [36], the deregulation of PI3K-mTOR and MAPK-related signaling has been linked to several clinically relevant disorders such as Alzheimer's disease and cancer [37, 38]. Thus, a thorough understanding of disease-specific mTOR-related signaling dynamics can provide valuable information in terms of potential drug targets [36]. Previously we combined highly selective phosphopeptide enrichment, based on Ti^{4+}-IMAC [39] with SRM to monitor and quantify crucial phosphosites of the PI3K-mTOR/MAPK pathway upon senescence [31]. The selection of these phosphosites of interest was based on extensive data mining in publicly available shotgun proteomics datasets, hence increasing the overall success rate of phosphopeptide SRM assay development. In the current study, we used these SRM assays, supplemented with MRM^3, to assess their performance compared to targeted data extraction, as used in DIA experiments. As a model system we chose nonsmall cell lung cancer cell lines (NSCLC), that were shown to rely highly on mTOR signaling (reviewed multiple times, most recently by Yip 2015 [40]). Especially in epidermal growth factor receptor (EGFR) tyrosine kinase inhibitor (TKI) resistant cell lines, NSCLC were shown to drastically differ in respect to their PI3K-mTOR/MAPK signaling compared to sensitive cell lines [41]. For this study, we chose to compare two NSCLC lines, PC9 that is sensitive to TKI treatment and H1975, which has T790M-mediated resistance to first-generation TKIs [42]. Combining highly selective phosphopeptide enrichment with SRM, DIA, and MRM^3 enabled us to determine the specific performance characteristics for these three MS acquisition modes as well as to gain insight into the mTOR signaling dynamics of different NSCLC lines.

2 Materials and methods

2.1 Cell culture

PC9 and H1975 NSCLC cells were purchased from Sigma-Aldrich and the American Type Culture Collection, respectively. PC9 cells contain a deletion (DelE746A750), where H1975 cells contain both the L858R and T780M mutations in the EGFR. Both cell lines were cultured in triplicates in standard Roswell Park Memorial Institute medium 1640 medium (Lonza), containing 10% FBS (Thermo), 2 mM L-glutamine and 1% penicillin/streptomycin (Lonza), at 37°C in a humidified atmosphere containing 5% CO_2.

Cells were detached from the culture surface using trypsin (Lonza), and washed three times with PBS before lysis. Drug response of both cell lines was tested as described in the Supporting Information.

2.2 Sample preparation and phosphopeptide enrichment

Frozen cell pellets were subjected to standard phosphoproteomic sample preparation as described before [31]. In brief the protocol combined cell lysis by sonication in urea-based lysis buffer, protein reduction (DTT), and alkylation (iodoacetamide) followed by Lys-C/Trypsin double digestion and desalting. Prior to phosphopeptide enrichment samples subjected to SRM measurements were split in two series and complemented with heavy isotope-labeled standard peptides (JPT) at concentrations of 150 fmol/mg lysate and 3 pmol/mg lysate, respectively. For each mass spectrometric measurement 300 μg lysate were enriched for phosphopeptides using Ti^{4+}-IMAC columns. For each biological replicate two phosphopeptide enrichment replicas per measurement methods were prepared. Further details about sample preparation are provided in the Supporting Information, including a detailed scheme about biological and technical replicas prepared for each acquisition method depicted in Supporting Information Fig. 1.

2.3 SRM measurements

Unless otherwise stated, all SRM experiments were conducted on a TSQ-Vantage (Thermo Fisher). Chromatographic separation was performed using an EASY-spray system containing an Easy-nLC 1000 coupled to a 25 cm, 75 μm ID PepMap RLSC, C18, 100 Å, 2 μm particle size column (Thermo Scientific, Odense, DK). SRM assays were adapted and extended from de Graaf et al. [31] including values for optimized collision energy. Phosphopeptides were separated on a gradient from 0 to 25% B in 170 minutes. The expected retention time of each peptide was determined from heavy isotope-labeled standard peptides analyzed in multiple unscheduled measurements. Endogenous phosphopeptides were measured in scheduled acquisition mode (10 min RT window, 4 s cycle time, 971 transitions in total reaching a maximum number of 173 concurrent transitions at RT = 65.90–65.98 min). Resolution was set to 0.7 Da peak width (fwhm) for both Q1 and Q3. Collision gas pressure was set to a constant value of 1.5 mTorr. Further Details about LC-MS/MS setup are provided in the Supporting Information.

2.4 MRM^3 measurements

All MRM^3 measurements were performed on an ekspert nano-LC 425 (Eksigent) coupled to a QTRAP 6500 (SCIEX). LC separation was carried out using a nanoAcquity (75 μm x 25 cm, 1.8 mm, HSS T3) column with a nanoAcquity (180 μm x 20 mm, 5μm Symmetry C18) trap column (Waters) in trap-elute configuration. Detailed information about instrument setup and acquisition methods are provided in the Supporting Information.

2.5 High pH-fractionation

A total of 4 mg cell digest mixed from both cell lines was fractionated on a high-pH (HpH) reversed-phase C18 column

(Gemini 3u C18 110 Å, 100 × 1.0 mm, Phenomenex) coupled to an Agilent 1100 series (Agilent Technologies) on a 60 min gradient. 67 fractions of 1 min each were collected and concatenated into five pools as previously described [43]. These were dried down in vacuo and subjected to phosphopeptide enrichment as described above, loading 1/3 of each fraction onto the Ti^{4+}-IMAC tip.

2.6 DIA library generation

Spectral libraries were acquired on a TripleTOF 5600 mass spectrometer (SCIEX) operated in data-dependent acquisition (DDA) mode. Upfront chromatographic separation was performed using an Agilent 1290 Infinity System (Agilent Technologies), adapted to nanoflow conditions by using a split flow setup as described in [44], coupled to in-house packed trap column (Dr. Maisch Reprosil C18, 3 μm, 2 cm × 100 μm) and analytical column (Agilent Poroshell 120 EC-C18, 2.7 μm, 50 cm × 75 μm) using a 155 min gradient. Further details about LC-MS/MS setup and detailed DDA criteria are provided in the Supporting Information.

2.7 DIA measurements

DIA measurements were acquired on a TripleTOF 5600 using the same instrument setup and gradients as described above. We used 64 variable DIA windows, each with 1 amu overlap (Supporting Information Fig. 2) spanning an *m/z* range of 400–1250. The collision energy for each window was determined based on the collision energy for a 2+ ion with a collision energy spread of 0 eV. An accumulation time of 50 ms was used for each fragment ion scan which in combination with a 100 ms survey scan resulted in a total cycle time of 3.4 s.

2.8 Data analysis

All SRM experiments were analyzed using Skyline [45]. To ensure reliable assessment of the SRM traces, signals were validated using mProphet [46], as implemented in the advanced peak picking option of Skyline. Decoy sequences were created by sequence shuffling and adding a precursor mass shift of 10 Da and measured in the same retention time window as their respective target peptide. The mProphet scoring model for SRM data was optimized according to an initial training sample and used without further optimization on all samples using a *q*-value cutoff of 0.01 (corresponding to a 1% FDR).

For DIA targeted data extraction, DDA measurements were searched using MASCOT [47] and combined to a spectral library in Skyline as described in more detail in the Supporting Information. Subsequent to targeted data extraction of both target and decoy sequences in Skyline, the DIA data

were validated using an mProphet scoring model directly optimized on the data. Compared to the model used for SRM it also contained DIA-specific scoring features such as mass errors and precursor isotope dot products. Specific mProphet feature scores and score distributions for both SRM and DIA data can be found in Supporting Information Table 1 and Supporting Information Fig. 3.

In both, SRM and DIA a few obvious wrongly assigned peaks were integrated manually, as indicated in Supporting Information Table 2.

Quantification was performed by integrating chromatographic fragment ion peak areas in Skyline. Pearson correlations were calculated and visualized with Perseus using intensity values for all transitions individually. CVs were determined by Skyline. Quantitative values were subsequently submitted to significance analysis using MSStats [48]. For SRM this included transforming ratios between analyte and internal standard to a $\log_2$-scale, for DIA global intensity normalization based on equalizing medians was performed, followed by $\log_2$-transformation of the intensity values. Peak groups not significantly annotated by mProphet were treated as missing values. A linear-mixed effects model was successively used to test for abundance changes between different cell lines. An FDR cutoff of ≤ 5% was considered significant. A list of the number of transitions used for each peptide for quantification and significance analysis is provided in Supporting Information Table 3.

3   Results and discussion

Here, we set out to assess and compare the performance of SRM, MRM[3], and DIA for MS-based targeted phosphoproteomics (Fig. 1). As model system we chose two different NSCLC lines, namely H1975 and PC9 that differ substantially in sensitivity to EGFR tyrosine kinase inhibitors. In these cells, we monitored phosphorylation events involved in PI3K-mTOR/MAPK signaling. Both cell lines were grown in triplicates and tested for their sensitivity to Gefitinib and Afatinib. As expected, H1975 showed increased tolerance toward both tyrosine kinase inhibitors (Supporting Information Fig. 4). All cells were subjected to alike sample preparation protocols (differing mainly in the amount of internal standards added in SRM) including the workflows used for tryptic digestion and subsequent phosphopeptide enrichment by Ti^{4+}-IMAC. For each biological replicate, two enrichment replicates for each MS method were prepared. A schematic of the sample preparation is depicted in Supporting Information Fig. 1. In Supporting Information Fig. 5 and 6 we show representative chromatographic elution profiles and information about retention time reproducibility for SRM and DIA, respectively. For SRM and DIA the maximal retention time shift is in the range of a minute within a 3 h gradient. Peak width in the SRM measurements range from 40 to 60 s and in DIA from roughly 30–120 s. Pearson correlations as well as CVs for each peptide are given in Supporting Information Fig. 7.
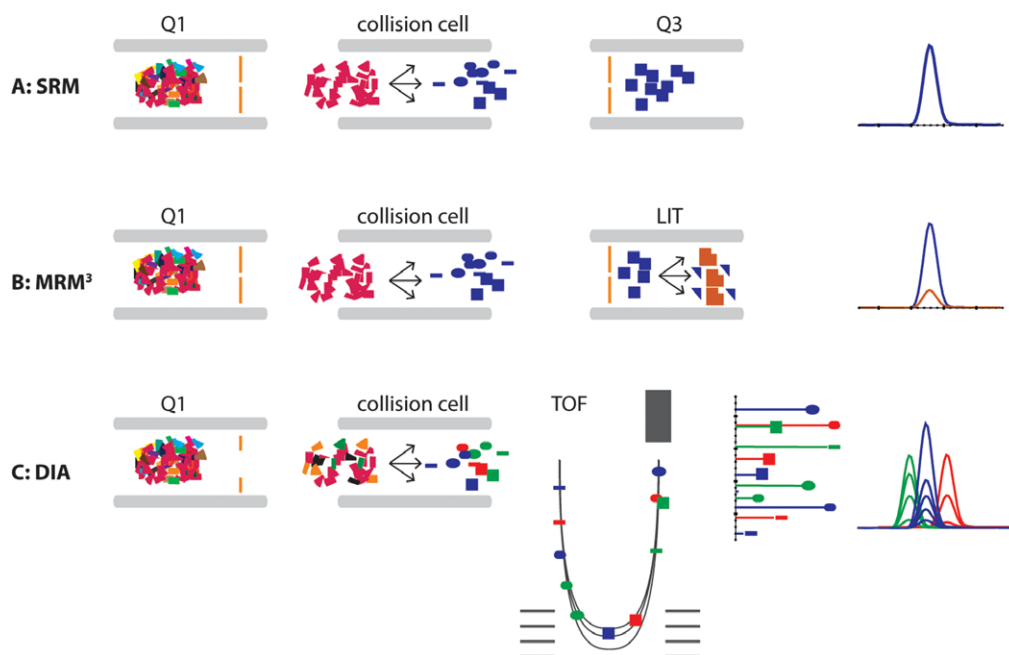
Figure 1. Schematic overview of three different MS-based targeted proteomics acquisition types evaluated for their application in phosphoproteomics. (A) In a triple quadrupole mass spectrometer SRM combines specific sets of *m/z* filters for Q1 and Q3, representing highly specific precursor and fragment ions pairs, so called transitions. Chromatographic traces of these transitions are then recorded for a predefined retention time window. (B) Compared to SRM, MRM³ adds an additional fragmentation and filtering event monitoring also chromatographic traces of secondary fragment ions. (C) DIA combines wide isolation windows for precursor *m/z* selection with acquisition of high-resolution fragmentation spectra. The resulting highly multiplexed fragmentation spectra are subsequently analyzed by targeted data extraction based on prior established spectral libraries.

3.1 Signal transduction monitoring by SRM

One of the major strengths of MS-based targeted proteomics is the capability to monitor specific molecular events of interest. In the case of phosphoproteomics, many global studies have been performed that give rise to large numbers of identified phosphosites [8, 9, 49, 50]. These studies give a global picture of phosphoproteome regulation, however, often lack the ability to comprehensively map all important phosphosites with reported function in signaling cascades or biological processes, caused by undersampling or lack of sensitivity. Here, we selected specific phosphorylation sites known to play important roles in the PI3K/mTOR and MAPK pathways as well as sites of so far unknown function, quantified in our earlier study [31] (Supporting Information Table 2). Sites of known function included activity inducing sites for the kinases AMPK-B1 (serine 108 [51]), PDK1 (serine 241 [52]), ERK1/2 (tyrosine 204 and 187, respectively [53]), p70S6K (serine 447 [54]), BRAF (serine 446 and serine 729 [55,56]) and mTOR (serine 1291 [57]) as well as kinase activity inhibiting phosphorylation sites for CDK1 (threonine 14 [58]), c-RAF (threonine 259 [59]), and IRS1 (serine 1101 [60]). Additionally several phosphosites were monitored, which are not located on kinases but have established roles in signal transmission. These sites included phosphorylation of serine 65 of

4EBP1, triggering the release of EIF4B to an unbound state and thus activating translation and protein synthesis [61], two phosphorylation sites of Akt1S1 that promote its dissociation from mTORC1 and consequently repress its inhibitory function on mTORC1 kinase activity [62–64], RAPTOR serine 863 which, upon phosphorylation induces mTORC1 activity [65] and PIK3C2A serine 259, where phosphorylation promotes its own degradation [66].

To accurately quantify the selected phosphosites, heavy isotope-labeled standard peptides were added after cell lysis and tryptic digestion in two different concentrations (150 fmol/mg proteins and 3 pmol/mg proteins), following a workflow presented earlier by de Graaf et al. [31], after which cell lysates were subjected to Ti⁴⁺-IMAC enrichment in duplicate for each of the two heavy isotope-labeled standard peptide concentrations. In total 48 phosphopeptides of the PI3K-mTOR/MAPK pathways were targeted by SRM. Based on mProphet scoring and manual data assessment, 40 of these targeted peptides could be significantly (mProphet *q*-value ≤ 0.01) detected in at least three out of six injections per cell line (Fig. 2).

An exceptional case is the phosphorylation of serine 415 of RSK2, which according to mProphet, has been confidently identified in all three biological replicas (including both enrichment replicas for each) of H1975 but only in one
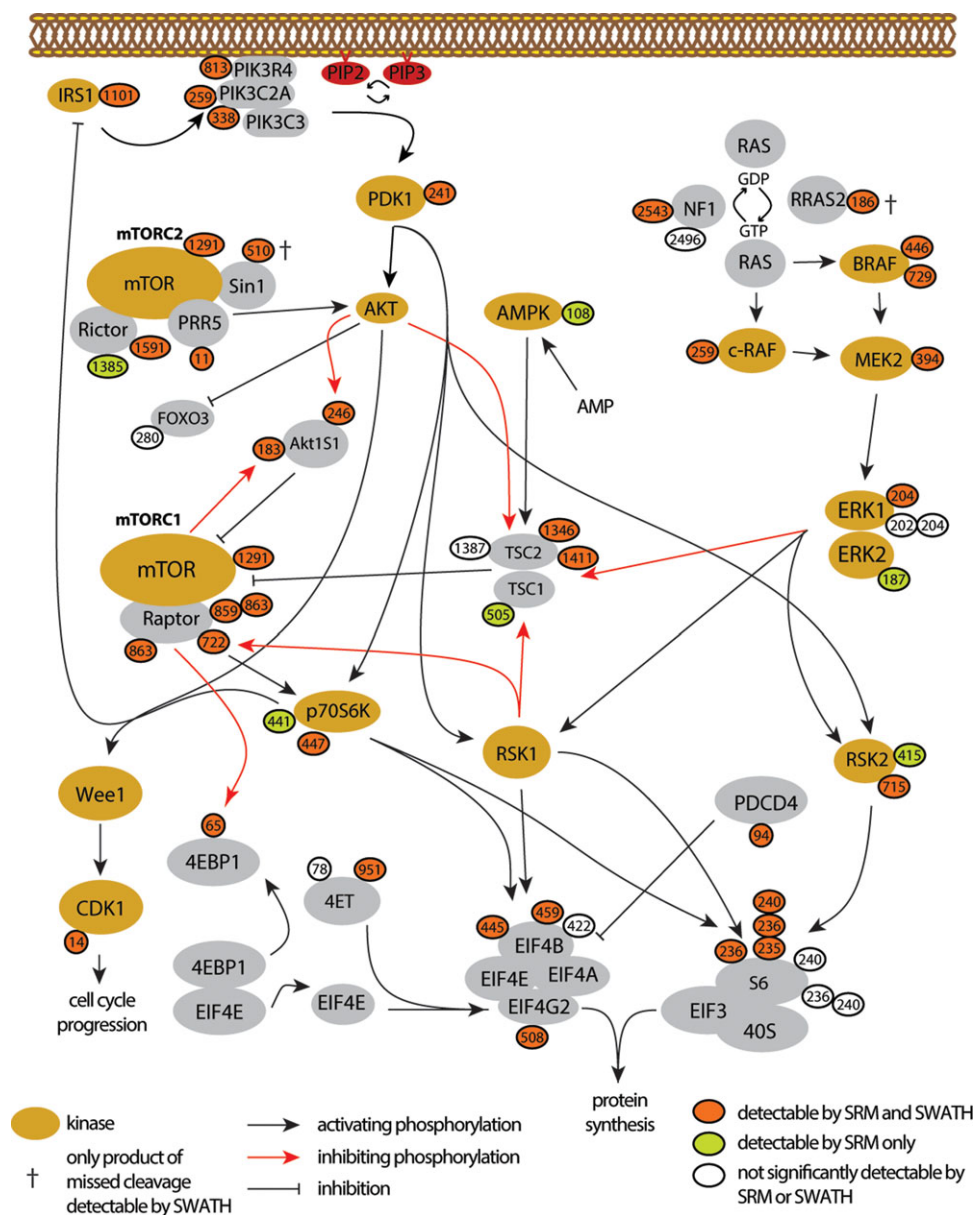
Figure 2. Overview of the detectability of phosphosites in the PI3K-mTOR/MAPK pathway in non-small cell lung cancer cell lines. Thirty-four phosphosites (orange) were significantly detected with SRM as well as DIA. For two phosphosites (Sin1 S510 and RRAS2 S186 (†)) only an alternative peptide containing a missed cleavage was detectable in DIA. Six additional phosphosites (light green) could be confidently detected by SRM but not by DIA. In case of phosphorylation site S415 in RSK2 detection was only successful in the H1975 cells.

enrichment replicate of PC9. Manual assessment of the data revealed consistent presence of the heavy isotope-labeled standard peptides across all samples. Peak groups for the endogenous peptide were detected in all replicas of H1975, whereas they hardly exceeded the noise threshold in PC9, thus suggesting a potential on/off situation for this particular phosphosite (Supporting Information Fig. 8).

3.2 MRM cubed

To increase our signaling pathway coverage we explored the use of MRM³ for targeted quantification of phosphosites. In

a previous study, Bauer et al. [25] showed increased sensitivity by performing MS3 on the neutral loss ion of low abundant phosphopeptides in a pseudo SRM approach, in the linear iontrap of an LTQ-Orbitrap. As a first proof of principle we selected two phosphopeptides from an existing dataset that performed poorly under "normal" optimized SRM conditions and developed MRM³ assays. One phosphopeptide (IS-(pho)S-PTETER) was selected based on an occurring interference and one (ALVHQL-(pho)S-NESR) based on its low S/N level. As can be seen in Supporting Information Fig. 9, for both these phosphopeptides MRM³ was able to drastically reduce interferences and improve the S/N levels. Based on these promising results we selected three specific
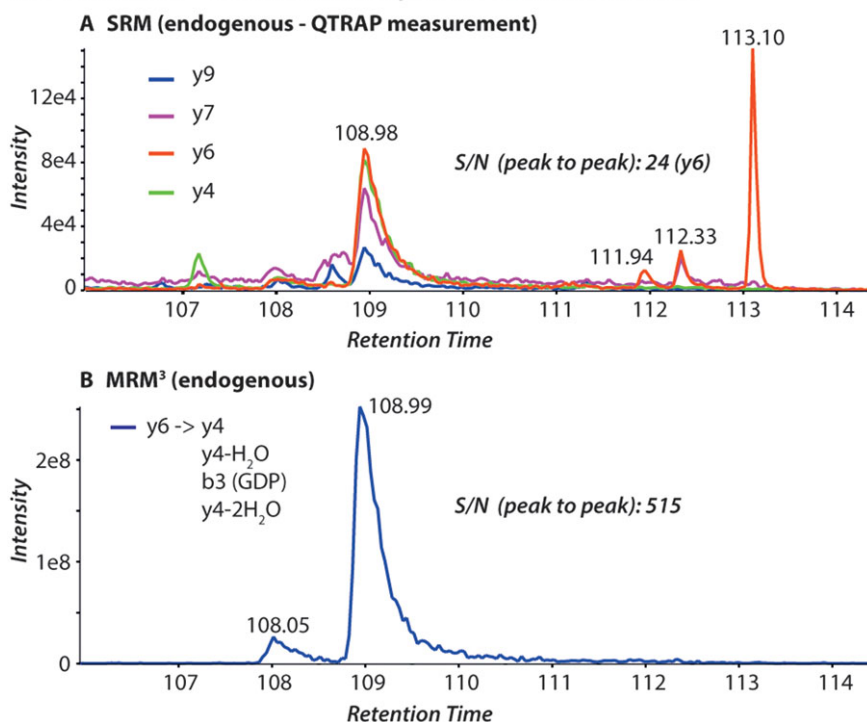
SRM versus MRM³ - TSC2 (S1387) : SS-(pho)S-SPELQTLQDILGDPGDK

Figure 3. Illustrative chromatographic traces obtained for the phosphopeptide SS-(pho)S-SPELQTLQDILGDPGDK measured in a complex cell lysate using two different measurement methods: (A) SRM and (B) MRM³ were acquired using the same instrument setup (QTRAP 6500). Compared to conventional SRM, MRM³ is capable of reducing unspecific ion signals, as seen by the disappearance of the peak groups at retention times 107.1, 111.9, 112.3, and 113.1 in the MRM³ workflow. For MRM³ longer accumulation times in the trap also enable a drastic increase in sensitivity, improving the S/N by a factor of more than 40.

phosphosites from the mTOR/PI3K pathway, with again either high interference or very low S/N ratio, to be targeted by MRM³, specifically PIK3R4 (S813), FOXO3 (S280), and TSC2 (S1387), with the latter two not accessible in our SRM experiments. The MRM³ experiments require MS instrumentation with trapping capabilities and were performed on a QTRAP 6500. Existing SRM assays were copied and reoptimized on the QTRAP, where the different LC-MS setup caused slightly different results, already in SRM mode. Still the selected sites performed poorly, as can be seen from TSC2 (S1387) in Fig. 3A. Likewise the other two sites showed very low S/N (Supporting Information Fig. 10). Next, these selected peptides were analyzed in MRM³ mode, optimizing crucial instrument parameters such as secondary ion selection, linear ion-trap fill time and excitation energy (Supporting Information Table 4). With this approach we were able to substantially increase the assay quality for those three phosphopeptides in terms of interference and sensitivity (Fig. 3B), expanding the coverage of nodes in the signal transduction cascade to 42 out of 48 targeted phosphopeptides. These results demonstrate the great potential of MRM³ analysis of (low abundant) phosphosites. However, due to the increased measurement time required (acquisition times of up to 1 s for MRM³), and the (so far) limited software support for scheduled MRM³ methods, comprehensive pathway analysis by MRM³ is not yet feasible. Yet, for most of the phosphosites investigated here this is not required as they perform well under SRM conditions. Thus we concluded that MRM³ is best used as a comple-

mentary method in combination with SRM, in which MRM³ is used specifically for a limited number of individual targets poorly detectable in SRM. A prerequisite for successful MRM³, however, is a sufficiently efficient secondary peptide fragmentation event (MS3). The fragment ion usually giving rise to the most informative MS3 spectra is the neutral loss of phosphoric acid. However, we found the SRM trace resulting from neutral loss of phosphoric acid to be nonspecific. Accordingly, the gain in specificity associated with the second fragmentation step in MRM³ was greatly reduced when targeting the neutral loss fragment, providing little increase in sensitivity or specificity over the best performing SRM traces (Supporting Information Fig. 11).

3.3 Signal transduction monitoring by data-independent acquisition

Next, we assessed the performance of DIA for the targeted analysis of the same 48 phosphopeptides, targeted by combining SRM and MRM³. The acquisition of a reference spectral library is an essential step for the targeted data extraction in DIA measurements. Here, we compared two different ways of acquiring this spectral library (Fig. 4A). So far the most promising approaches described in literature include pooling all samples of interest followed by extensive fractionation [67, 68]. In view of these results, we performed high-pH reversed-phase (HpH) fractionation with subsequent phosphopeptide
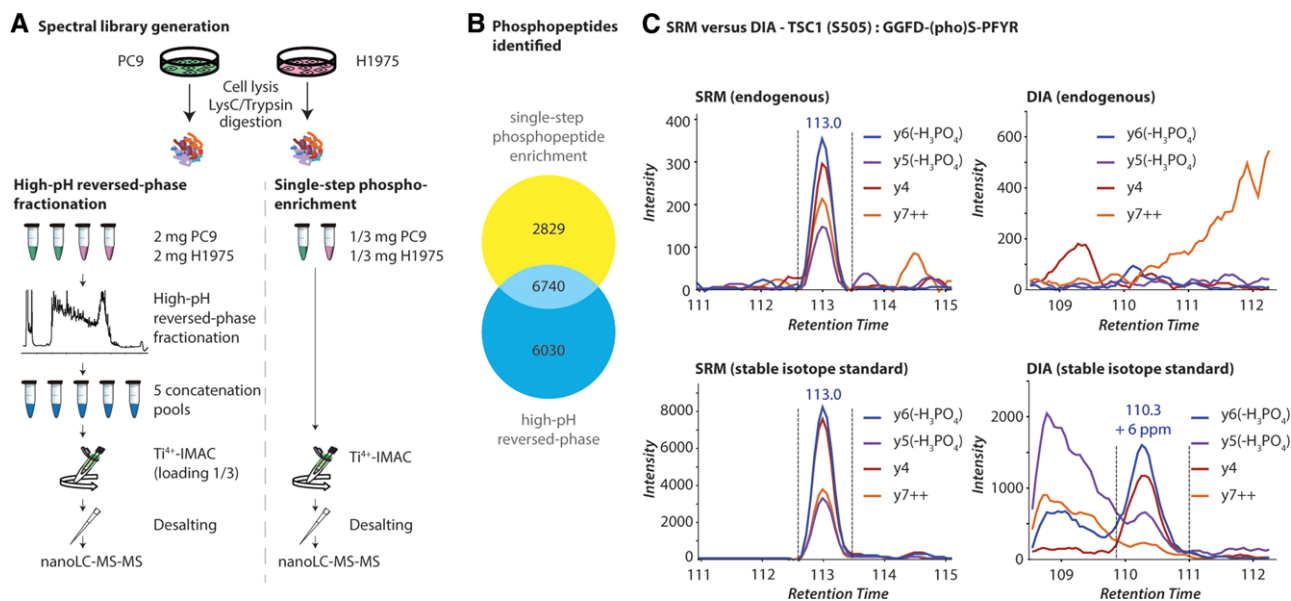
Figure 4. (A) Build-up of spectral libraries for the DIA analysis using two different strategies: Either pooled peptide digest of PC9 and H1975 cell lines were fractionated using high-pH reversed-phase chromatography and concatenated to five fractions followed by phosphopeptide enrichment (left side) or the digest of both cell lines were directly enriched (right side) after which samples were analyzed by DDA. (B) Venn diagram comparing the number of unique phosphopeptides identified in the two spectral libraries. (C) The reduced sensitivity of DIA compared to SRM exemplified by the phosphopeptide GGFD-(pho)S-PFYR. Samples for both measurements contained equal amounts of heavy isotope-labeled standard peptides for this example. Panels show chromatographic traces for SRM (left panels) and DIA (right panels), endogenous peptides (upper panels) and stable isotope standard (lower panels).

enrichment on a mixed PC9 and H1975 cell lysate. Using a concatenation strategy as demonstrated by Batth et al. [43] we identified 12 770 phosphopeptides from 5 HpH fractions. To investigate if the increased proteomic depth of the library benefits the targeted data extraction we decided to acquire a second spectral library combining one single (unfractionated) DDA analysis of each cell line only, giving rise to a combined library containing 9569 phosphopeptides. Figure 4B shows the overlap between these two spectral libraries, with, as expected, the highest number of unique phosphosites in the HpH-generated library. Subsequently, similar as in the above-described SRM experiments, two Ti⁴⁺-IMAC enrichments per biological replicate were prepared and analyzed in DIA mode. Based on the acquired spectral libraries, mProphet scoring and visual assessment of the DIA data, we were able to extract peak groups for 34 of the 48 phosphosites targeted by SRM (Fig. 2). Thirty-three out of the 34 peptides detected by DIA could be observed in the smaller spectral library already.

3.4 Comparison between SRM and DIA in terms of sensitivity

The initial DIA study by Gillet et al. reported an approximately tenfold lower sensitivity of DIA compared to SRM, based on classical dilution curve experiments [27]. In this study, we

show potential implications of this loss in sensitivity when aiming for comprehensive pathway analysis. Six phospho-sites within the mTOR signaling network that were well accessible by optimized SRM assays remained inaccessible for DIA analysis, hence limiting information about pathway dynamics. To illustrate this loss in sensitivity, chromatographic traces of TSC1 (S505) measured in SRM and DIA are displayed in Fig. 4C. To ensure an unbiased evaluation, SRM and DIA measurements were both performed on PC9 samples containing 50 fmol of the heavy isotope-labeled standard phosphopeptides. The synthetic peptide clearly shows the difference in sensitivity (in S/N) between SRM and DIA for this specific phosphopeptide. For the endogenous phosphopeptide this difference in sensitivity between the two methods leads to a situation in which a clear signal can be obtained with SRM whereas it remains below detection limit for DIA. In two other cases, specific phosphopeptides successfully targeted by SRM were not detectable by DIA, however, the phosphosites could be quantified by extracting peak groups for their corresponding phosphopeptides containing missed cleavages. This again highlights the difference in sensitivity between the two methods, but also demonstrates the benefit of DIA when it comes to target peptide selection. Whereas in DIA it is straightforward to refine the target peptide selection postacquisition this would require de novo assay development and data acquisition in SRM.
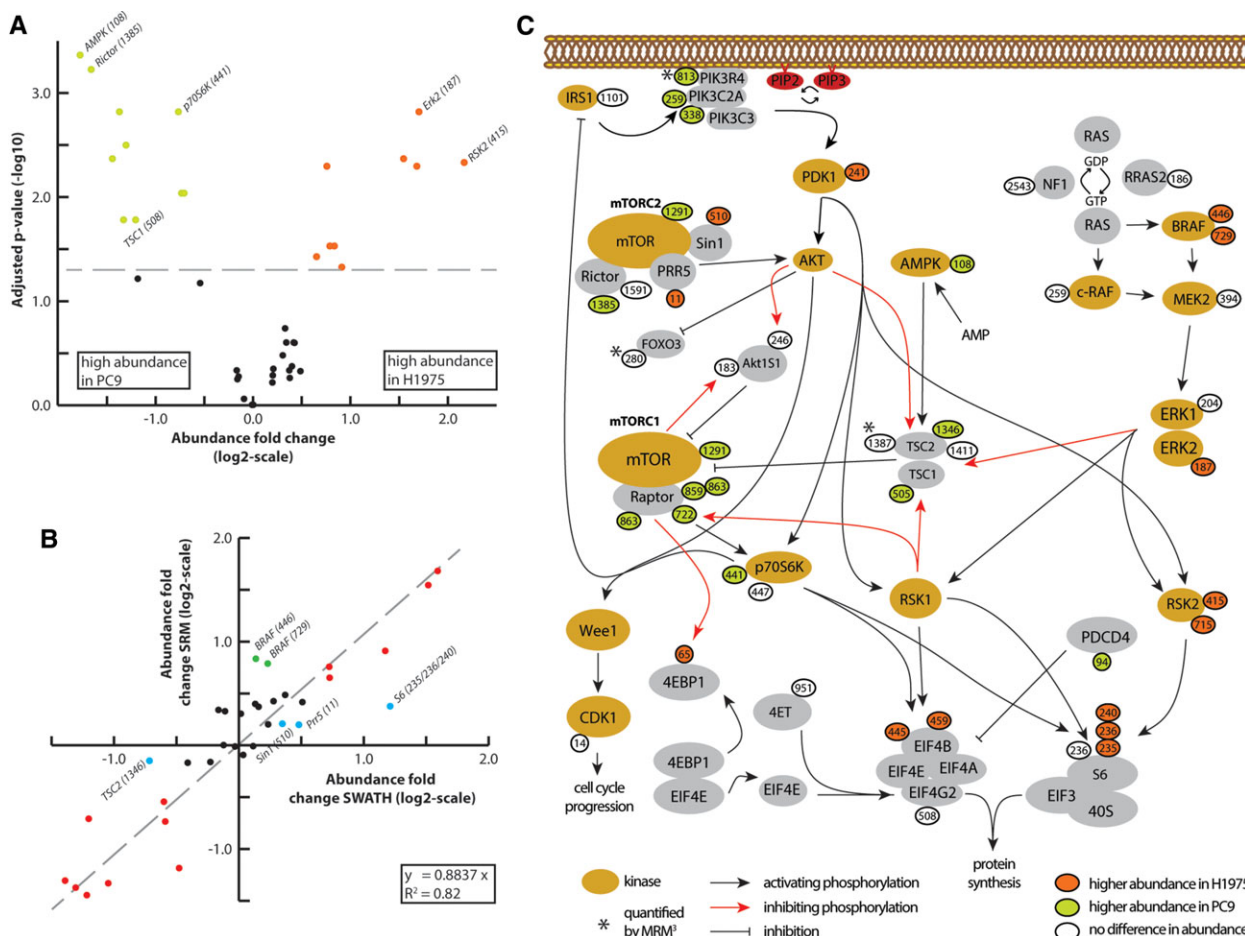
Figure 5. (A) Statistical analysis of the differential abundances of the detected phosphopeptides between H1975 cells and PC9 cells as detected by SRM displayed in a volcano plot. *p* values (–log$_{10}$ of adjusted *p*-value) are plotted as a function of the differential abundance observed using $p \leq 0.05$ as significance threshold. Significant changes in abundance are color coded (orange = higher abundance in H1975, light green = higher abundance in PC9). Labeled dots represent phosphosites not accessible by DIA. (B) Correlation between phosphopeptide abundance differences as determined by DIA and SRM. Abundance fold changes are defined as log$_2$ (abundance$_{H1975}$/abundance$_{PC9}$). Values in red represent a significant ($p \leq 0.05$) differential abundance observed with both methods, dots marked in green and blue represent significant fold changes exclusively determined by SRM and DIA, respectively. (C) Phosphosite localization within the PI3K/mTOR/MAPK signaling pathway, color coded by abundance changes between H1975 cells and PC9 cells ($p \leq 0.05$).

3.5 Quantification of PI3K/mTOR and MAPK phosphosites

Both the SRM dataset and the DIA dataset were separately tested to determine significant changes in abundance between the two cell lines (numeric results are provided in Supporting Information Table 5). Figure 5A depicts the results obtained from the SRM experiments. The volcano plot shows several phosphosites exhibiting significant differential abundances between the two investigated cell lines, with those annotated with their protein name uniquely quantified by SRM. Comparison of the quantification results obtained with SRM and DIA shows a reasonably good correlation ($R^2 = 0.82$, Fig. 5B), although lower than reported by Gillet et al. ($R^2 = 0.95$). This is mainly caused by two phosphosites (BRAF) exclusively regulated in the SRM experiment, and

four regulated phosphosites exclusive to the DIA experiment. This discrepancy between the previously obtained correlation and the one reported here likely originates from the fact that (1) the previously reported SRM and DIA correlation was obtained at protein level analysis, generally involving more than one peptide per protein, thus strengthening the reliability of the quantification. (2) The quantitative fold changes reported here are relatively small, up to fourfold maximum, whereas Gillet et al. reported fold changes of up to 300. Overall the observed differences are small and both SRM and DIA largely agree quantitatively.

Of note, in some cases multiple potential peak groups show up in both SRM and DIA data (Supporting Information Fig. 12). This might be caused by potential different phosphorylation sites on the same peptide, which do share most of the transitions but differ slightly in retention time.

For an automated peak picking and scoring program such as mProphet or Spectronaut distinction of such features is highly challenging, demonstrating the importance of manual data assessment in both SRM and DIA, in particular when analyzing phosphopeptides.

Quantification by MRM[3] could confirm the significantly higher abundance of PIK3R4 (S813) in PC9, as previously determined by both SRM and DIA. For the remaining two phosphopeptides targeted by MRM[3] no significant difference in abundance across the two cell lines was observed (Supporting Information Table 6).

3.6 Implications of TKI resistance on mTOR signaling

We quantified 42 phosphopeptides across two different non-small cell lung cancer cell lines using three different MS-based targeted proteomics approaches. Of these monitored phosphosites, 25 showed significant differential regulation between the two cell lines, 12 displaying an increased and 13 a decreased abundance in H1975 compared to PC9 (Fig. 5C). Overall the differences in phosphosite abundances observed here suggest a more complex change in mTOR signaling between the two cell lines than a mere up- or downregulation of the whole pathway. It is striking that many phosphosites in the downstream region of the signaling pathway clearly suggest an elevated rate of protein synthesis in H1975 compared to PC9. This begins with phosphorylation of S65 of 4EBP1 releasing EIF4E to activate translation, followed by an increase in phosphorylation of S445 and S459 on EIF4B. Moreover, the phosphorylation of PDCD4 at serine 94 showed a decreased abundance in H1975 compared to PC9. PDCD4 has been shown to inhibit protein translation but gets rapidly degraded in proliferating cells [69], hence the decrease in abundance of its phosphorylation, caused by protein degradation, corroborating a potential increase in protein synthesis. In line with these observations, we find the abundance of ERK2 S187 and the two phosphosites of RSK2 to be more abundant upon TKI resistance (with RSK S415 exclusively present in H1975), which again is consistent with an increase in protein synthesis. It is however interesting that the entire BRAF/MAPK pathway upstream of ERK2 does not show any difference in abundance between the two cell lines, except for a slight up-regulation of BRAF detected in SRM but not confirmed by DIA.

Remarkably, many other phosphosites localized in upstream regions of the PI3K-mTOR pathway show opposing trends, namely higher abundance in the TKI sensitive PC9 cells. These sites include several phosphosites in the mTORC1 pathways as well as the phosphoinositide 3-kinase (PI3K) complex. It has been shown in previous studies performed on tumor biopsies of patients treated with mTORC1 inhibitors, that there is a negative feedback loop between activation of PI3K/mTORC1 and the MAPK pathway [70] suggesting a certain negative cross-control between the two

prosurvival pathways. An opposing trend in the two pathways as observed in our data is therefore plausible and might be part of two different prosurvival mechanisms.

In many cases, we observed that multiple phosphosites on the same protein, or in case of mTORC1 and PI3K the same protein complex, show very similar quantitative behavior (summarized in Supporting Information Table 7). This suggests that molecular changes rather happen at the protein expression than protein phosphorylation level. In a study on the effects of TKI resistance on mTOR signaling, Fei et al. detected substantial difference in kinase activity between mTORC1 and mTORC2 in different NSCLC lines [41]. Using a combination of pull downs and in vitro kinase assays they observed an increased kinase activity of mTORC2 in TKI resistant cells as well as an increased kinase activity of mTORC1 in TKI sensitive cells, which nicely is in accordance with our present study.

4   Concluding remarks

MS-based targeted proteomics has become a valuable proteomics tool including its current variants SRM, MRM[3], and DIA. In this study, we evaluated the performance of these three popular methods for the targeted analysis of phosphorylation events in specific signaling networks. By monitoring the PI3K-mTOR/MAPK pathway dynamics in different NSCLC cell lines we could pinpoint advantages and disadvantages of all three methods. SRM outperforms DIA in terms of sensitivity resulting in increased pathway coverage by approximately 15%. DIA, however, exceeds SRM in terms of flexibility, as shown here by quantifying alternative tryptic cleavage products, a strategy that would involve tedious de novo assay development in SRM. By quantifying three phosphosites using MRM[3] we show the additional benefit of this feature over a conventional SRM assay in terms of sensitivity and selectivity, increasing the phosphopeptide coverage in our selected pathway even further.

These considerations can be of great value for successful experiment planning, as all three methods can prove optimal depending on the specific question asked and the resources available. In a purely hypothesis-driven approach, SRM (likely in combination with MRM[3]) is likely still the most promising approach, although it comes at the cost of time-consuming assay development and the requirement of heavy isotope-labeled standard peptides for each analyte of interest. In exchange all parameters such as collision energy or dwell time can be iteratively optimized for each transition individually, resulting in highly sensitive assays. In DIA internal standards are mostly omitted, mainly because the measurement of a survey scan enables very robust normalization based on total ion signal as implemented in many label-free shotgun quantification approaches. This renders DIA the cheaper method in terms of both cost and time. However, the unspecific isolation windows and the acquisition of

full-scan MS/MS spectra result in way more restrictions in terms of parameter optimization for DIA compared to SRM, which is one of the reasons for the lower sensitivity compared to SRM.

Next to the reduced sensitivity one of the biggest disadvantages of DIA is the requirement of a spectral library, which is time consuming to build. However, the increasing availability of proteomics sequencing data in online repositories might rapidly overcome this disadvantage in the near future. Hence, our observations suggest a great potential for DIA to grow to an "easy to use" alternative to SRM, if the cost of reduced sensitivity does not conflict with the question at hand. Moreover, it remains to be seen whether DIA approaches can outperform "single shot" label-free quantification in terms of quantitative depth and throughput [71].

Using MS-based targeted proteomics on phosphopeptides does pose additional challenges, especially in terms of peak picking, which requires a thorough manual data assessment in addition to automatized data analysis pipelines such as mProphet or Spectronaut. Nonetheless, the three methods described here all exhibit great potential for accurate quantification, showing sufficient reproducibility between different measurement strategies. Thus, altogether our data shows that MS-based targeted proteomics methods have matured, allowing the measurement of even subtle differences in protein phosphorylation.

Associated Contend

Raw data can be found in http://www.peptideatlas.org/PASS/PASS00770 including:

- Raw files (SRM), wiff files (DIA, MRM3).
- Skyline daily files for SRM (two different concentrations of heavy isotope-labeled standard peptides) and DIA including mProphet scores.
- Transition lists for SRM and DIA.
- Raw quantitative values as exported from Skyline and subjected to MSStats analysis.

5 References

[1] White, F. M., Quantitative phosphoproteomic analysis of signaling network dynamics. *Curr. Opin. Biotechnol.* 2008, *19*, 404–409.

[2] Altelaar, A. F., Munoz, J., Heck, A. J., Next-generation proteomics: towards an integrative view of proteome dynamics. *Nat. Rev. Genet.* 2013, *14*, 35–48.

[3] Lemeer, S., Heck, A. J., The phosphoproteomics data explosion. *Curr. Opin. Chem. Biol.* 2009, *13*, 414–420.

[4] Macek, B., Mann, M., Olsen, J. V., Global and site-specific quantitative phosphoproteomics: principles and applications. *Annu. Rev. Pharmacol. Toxicol.* 2009, *49*, 199–221.

[5] Thingholm, T. E., Jensen, O. N., Larsen, M. R., Analytical strategies for phosphoproteomics. *Proteomics* 2009, *9*, 1451–1468.

[6] Riley, N. M., Coon, J. J., Phosphoproteomics in the age of rapid and deep proteome profiling. *Anal. Chem.* 2015, 88, *1*, 74–94.

[7] Giansanti, P., Aye, T. T., van den Toorn, H., Peng, M. et al., An augmented multiple-protease-based human phosphopeptide atlas. *Cell Rep.* 2015, 11, *11*, 1834–1843.

[8] de Graaf, E. L., Giansanti, P., Altelaar, A. F., Heck, A. J. et al., Single-step enrichment by Ti4+-IMAC and label-free quantitation enables in-depth monitoring of phosphorylation dynamics with high reproducibility and temporal resolution. *Mol. Cell. Proteomics* 2014, *13*, 2426–2434.

[9] Bodenmiller, B., Wanka, S., Kraft, C., Urban, J. et al., Phosphoproteomic analysis reveals interconnected system-wide responses to perturbations of kinases and phosphatases in yeast. *Sci. Signal.* 2010, *3*, rs4.

[10] Michalski, A., Cox, J., Mann, M., More than 100,000 detectable peptide species elute in single shotgun proteomics runs but the majority is inaccessible to data-dependent LC-MS/MS. *J. Proteome Res.* 2011, *10*, 1785–1793.

[11] Sajic, T., Liu, Y., Aebersold, R., Using data-independent, high-resolution mass spectrometry in protein biomarker research: perspectives and clinical applications. *Proteomics Clin. Appl.* 2015, *9*, 307–321.

[12] Picotti, P., Rinner, O., Stallmach, R., Dautel, F. et al., High-throughput generation of selected reaction-monitoring assays for proteins and proteomes. *Nat. Methods* 2010, *7*, 43–46.

[13] Gallien, S., Duriez, E., Crone, C., Kellmann, M. et al., Targeted proteomic quantification on quadrupole-orbitrap mass spectrometer. *Mol. Cell. Proteomics* 2012, *11*, 1709–1723.

[14] Peterson, A. C., Russell, J. D., Bailey, D. J., Westphall, M. S. et al., Parallel reaction monitoring for high resolution and high mass accuracy quantitative, targeted proteomics. *Mol. Cell. Proteomics* 2012, *11*, 1475–1488.

[15] Gallien, S., Domon, B., Detection and quantification of proteins in clinical samples using high resolution mass spectrometry. *Methods* 2015, *81*, 15–23.

[16] Tong, L., Zhou, X. Y., Jylha, A., Aapola, U. et al., Quantitation of 47 human tear proteins using high resolution multiple

reaction monitoring (HR-MRM) based-mass spectrometry. *J. Proteomics* 2015, *115*, 36–48.

[17] Gallien, S., Bourmaud, A., Kim, S. Y., Domon, B. et al., Technical considerations for large-scale parallel reaction monitoring analysis. *J. Proteomics* 2014, *100*, 147–159.

[18] Picotti, P., Aebersold, R., Selected reaction monitoring-based proteomics: workflows, potential, pitfalls and future directions. *Nat. Methods* 2012, *9*, 555–566.

[19] Jones, J. W., Pierzchalski, K., Yu, J., Kane, M. A. et al., Use of fast HPLC multiple reaction monitoring cubed for endogenous retinoic acid quantification in complex matrices. *Anal. Chem.* 2015, *87*, 3222–3230.

[20] Fortin, T., Salvador, A., Charrier, J. P., Lenz, C. et al., Multiple reaction monitoring cubed for protein quantification at the low nanogram/milliliter level in nondepleted human serum. *Anal. Chem.* 2009, *81*, 9343–9352.

[21] Lakowski, T. M., Szeitz, A., Pak, M. L., Thomas, D. et al., MS³ fragmentation patterns of monomethylarginine species and the quantification of all methylarginine species in yeast using MRM³. *J. Proteomics* 2013, *80*, 43–54.

[22] Lemoine, J., Fortin, T., Salvador, A., Jaffuel, A. et al., The current status of clinical proteomics and the use of MRM and MRM(3) for biomarker validation. *Expert. Rev. Mol. Diagn.* 2012, *12*, 333–342.

[23] Jaffuel, A., Lemoine, J., Aubert, C., Simon, R. et al., Optimization of liquid chromatography-multiple reaction monitoring cubed mass spectrometry assay for protein quantification: application to aquaporin-2 water channel in human urine. *J. Chromatogr. A* 2013, *1301*, 122–130.

[24] Jeudy, J., Salvador, A., Simon, R., Jaffuel, A. et al., Overcoming biofluid protein complexity during targeted mass spectrometry detection and quantification of protein biomarkers by MRM cubed (MRM3). *Anal. Bioanal. Chem.* 2014, *406*, 1193–1200.

[25] Bauer, M., Ahrné, E., Baron, A. P., Glatter, T. et al., Evaluation of data-dependent and -independent mass spectrometric workflows for sensitive quantification of proteins and phosphorylation sites. *J. Proteome Res.* 2014, *13*, 5973–5988.

[26] Venable, J. D., Dong, M. Q., Wohlschlegel, J., Dillin, A. et al., Automated approach for quantitative analysis of complex peptide mixtures from tandem mass spectra. *Nat. Methods* 2004, *1*, 39–45.

[27] Gillet, L. C., Navarro, P., Tate, S., Röst, H. et al., Targeted data extraction of the MS/MS spectra generated by data-independent acquisition: a new concept for consistent and accurate proteome analysis. *Mol. Cell. Proteomics* 2012, *11*, O111.016717.

[28] Röst, H. L., Rosenberger, G., Navarro, P., Gillet, L. et al., Open SWATH enables automated, targeted analysis of data-independent acquisition MS data. *Nat. Biotechnol.* 2014, *32*, 219–223.

[29] Unwin, R. D., Griffiths, J. R., Leverentz, M. K., Grallert, A. et al., Multiple reaction monitoring to identify sites of protein phosphorylation with high sensitivity. *Mol. Cell. Proteomics* 2005, *4*, 1134–1144.

[30] Wolf-Yadlin, A., Hautaniemi, S., Lauffenburger, D. A., White, F. M. et al., Multiple reaction monitoring for robust quantitative proteomic analysis of cellular signaling networks. *Proc. Natl. Acad. Sci. USA* 2007, *104*, 5860–5865.

[31] de Graaf, E. L., Kaplon, J., Mohammed, S., Vereijken, L. A. et al., Signal transduction reaction monitoring deciphers site-specific PI3K-mTOR/MAPK pathway dynamics in oncogene-induced senescence. *J. Proteome Res.* 2015, *14*, 2906–2914.

[32] Jin, L. L., Tong, J., Prakash, A., Peterman, S. M. et al., Measurement of protein phosphorylation stoichiometry by selected reaction monitoring mass spectrometry. *J. Proteome Res.* 2010, *9*, 2752–2761.

[33] Soste, M., Hrabakova, R., Wanka, S., Melnik, A. et al., A sentinel protein assay for simultaneously quantifying cellular processes. *Nat. Methods* 2014, *11*, 1045–1048.

[34] Zawadzka, A. M., Schilling, B., Held, J. M., Sahu, A. K. et al., Variation and quantification among a target set of phosphopeptides in human plasma by multiple reaction monitoring and SWATH-MS2 data-independent acquisition. *Electrophoresis* 2014, *35*, 3487–3497.

[35] Parker, B. L., Yang, G., Humphrey, S. J., Chaudhuri, R. et al., Targeted phosphoproteomics of insulin signaling using data-independent acquisition mass spectrometry. *Sci. Signal.* 2015, *8*, rs6.

[36] Chiarini, F., Evangelisti, C., McCubrey, J. A., Martelli, A. M. et al., Current treatment strategies for inhibiting mTOR in cancer. *Trends Pharmacol. Sci.* 2015, *36*, 124–135.

[37] Xu, K., Liu, P., Wei, W., mTOR signaling in tumorigenesis. *Biochim. Biophys. Acta.* 2014, *1846*, 638–654.

[38] Liko, D., Hall, M. N., mTOR in health and in sickness. *J. Mol. Med.* 2015, *93*, 1061–1073.

[39] Zhou, H., Ye, M., Dong, J., Corradini, E. et al., Robust phosphoproteome enrichment using monodisperse microsphere-based immobilized titanium (IV) ion affinity chromatography. *Nat. Protoc.* 2013, *8*, 461–480.

[40] Yip, P. Y., Phosphatidylinositol 3-kinase-AKT-mammalian target of rapamycin (PI3K-Akt-mTOR) signaling pathway in non-small cell lung cancer. *Transl. Lung Cancer Res.* 2015, *4*, 165–176.

[41] Fei, S. J., Zhang, X. C., Dong, S., Cheng, H. et al., Targeting mTOR to overcome epidermal growth factor receptor tyrosine kinase inhibitor resistance in non-small cell lung cancer cells. *PLoS One* 2013, *8*, e69104.

[42] Sharma, S. V., Bell, D. W., Settleman, J., Haber, D. A. et al., Epidermal growth factor receptor mutations in lung cancer. *Nat. Rev. Cancer* 2007, *7*, 169–181.

[43] Batth, T. S., Francavilla, C., Olsen, J. V., Off-line high-pH reversed-phase fractionation for in-depth phosphoproteomics. *J. Proteome Res.* 2014, *13*, 6176–6186.

[44] Cristobal, A., Hennrich, M. L., Giansanti, P., Goerdayal, S. S. et al., In-house construction of a UHPLC system enabling the identification of over 4000 protein groups in a single analysis. *Analyst* 2012, *137*, 3541–3548.

[45] MacLean, B., Tomazela, D. M., Shulman, N., Chambers, M. et al., Skyline: an open source document editor for creating and analyzing targeted proteomics experiments. *Bioinformatics* 2010, *26*, 966–968.

[46] Reiter, L., Rinner, O., Picotti, P., Hüttenhain, R. et al., mProphet: automated data processing and statistical validation for large-scale SRM experiments. *Nat. Methods* 2011, *8*, 430–435.

[47] Perkins, D. N., Pappin, D. J., Creasy, D. M., Cottrell, J. S. et al., Probability-based protein identification by searching sequence databases using mass spectrometry data. *Electrophoresis* 1999, *20*, 3551–3567.

[48] Chang, C. Y., Picotti, P., Hüttenhain, R., Heinzelmann-Schwarz, V. et al., Protein significance analysis in selected reaction monitoring (SRM) measurements. *Mol. Cell. Proteomics* 2012, *11*, M111.014662.

[49] Olsen, J. V., Blagoev, B., Gnad, F., Macek, B. et al., Global, in vivo, and site-specific phosphorylation dynamics in signaling networks. *Cell* 2006, *127*, 635–648.

[50] Smit, M. A., Maddalo, G., Greig, K., Raaijmakers, L. M. et al., ROCK1 is a potential combinatorial drug target for BRAF mutant melanoma. *Mol. Syst. Biol.* 2014, *10*, 772.

[51] Sanders, M. J., Ali, Z. S., Hegarty, B. D., Heath, R. et al., Defining the mechanism of activation of AMP-activated protein kinase by the small molecule A-769662, a member of the thienopyridone family. *J. Biol. Chem.* 2007, *282*, 32539–32548.

[52] Casamayor, A., Morrice, N. A., Alessi, D. R., Phosphorylation of Ser-241 is essential for the activity of 3-phosphoinositide-dependent protein kinase-1: identification of five sites of phosphorylation in vivo. *Biochem. J.* 1999, *342* (Pt 2), 287–292.

[53] Jurek, A., Amagasaki, K., Gembarska, A., Heldin, C. H. et al., Negative and positive regulation of MAPK phosphatase 3 controls platelet-derived growth factor-induced Erk activation. *J. Biol. Chem.* 2009, *284*, 4626–4634.

[54] Lekmine, F., Sassano, A., Uddin, S., Smith, J. et al., Interferon-gamma engages the p70 S6 kinase to regulate phosphorylation of the 40S S6 ribosomal protein. *Exp. Cell. Res.* 2004, *295*, 173–182.

[55] Tran, N. H., Wu, X., Frost, J. A., B-Raf and Raf-1 are regulated by distinct autoregulatory mechanisms. *J. Biol. Chem.* 2005, *280*, 16244–16253.

[56] MacNicol, M. C., Muslin, A. J., MacNicol, A. M., Disruption of the 14-3-3 binding site within the B-Raf kinase domain uncouples catalytic activity from PC12 cell differentiation. *J. Biol. Chem.* 2000, *275*, 3803–3809.

[57] Acosta-Jaquez, H. A., Keller, J. A., Foster, K. G., Ekim, B. et al., Site-specific mTOR phosphorylation promotes mTORC1-mediated signaling and cell growth. *Mol. Cell Biol.* 2009, *29*, 4308–4324.

[58] Chow, J. P., Siu, W. Y., Ho, H. T., Ma, K. H. et al., Differential contribution of inhibitory phosphorylation of CDC2 and CDK2 for unperturbed cell cycle control and DNA integrity checkpoints. *J. Biol. Chem.* 2003, *278*, 40815–40828.

[59] Kilili, G. K., Kyriakis, J. M., Mammalian Ste20-like kinase (Mst2) indirectly supports Raf-1/ERK pathway activity via maintenance of protein phosphatase-2A catalytic subunit levels and consequent suppression of inhibitory Raf-1 phosphorylation. *J. Biol. Chem.* 2010, *285*, 15076–15087.

[60] Li, Y., Soos, T. J., Li, X., Wu, J. et al., Protein kinase C Theta inhibits insulin signaling by phosphorylating IRS1 at Ser(1101). *J. Biol. Chem.* 2004, *279*, 45304–45307.

[61] Peter, D., Igreja, C., Weber, R., Wohlbold, L. et al., Molecular architecture of 4E-BP translational inhibitors bound to eIF4E. *Mol. Cell* 2015, *57*, 1074–1087.

[62] Vander Haar, E., Lee, S. I., Bandhakavi, S., Griffin, T. J. et al., Insulin signalling to mTOR mediated by the Akt/PKB substrate PRAS40. *Nat. Cell Biol.* 2007, *9*, 316–323.

[63] Wang, L., Harris, T. E., Roth, R. A., Lawrence, J. C. et al., PRAS40 regulates mTORC1 kinase activity by functioning as a direct inhibitor of substrate binding. *J. Biol. Chem.* 2007, *282*, 20036–20044.

[64] Wang, L., Harris, T. E., Lawrence, J. C., Regulation of proline-rich Akt substrate of 40 kDa (PRAS40) function by mammalian target of rapamycin complex 1 (mTORC1)-mediated phosphorylation. *J. Biol. Chem.* 2008, *283*, 15619–15627.

[65] Wu, X. N., Wang, X. K., Wu, S. Q., Lu, J. et al., Phosphorylation of raptor by p38beta participates in arsenite-induced mammalian target of rapamycin complex 1 (mTORC1) activation. *J. Biol. Chem.* 2011, *286*, 31501–31511.

[66] Didichenko, S. A., Fragoso, C. M., Thelen, M., Mitotic and stress-induced phosphorylation of HsPI3K-C2alpha targets the protein for degradation. *J. Biol. Chem.* 2003, *278*, 26055–26064.

[67] Zi, J., Zhang, S., Zhou, R., Zhou, B. et al., Expansion of the ion library for mining SWATH-MS data through fractionation proteomics. *Anal. Chem.* 2014, *86*, 7242–7246.

[68] Shao, S., Guo, T., Koh, C. C., Gillessen, S. et al., Minimal sample requirement for highly multiplexed protein quantification in cell lines and tissues by PCT-SWATH mass spectrometry. *Proteomics* 2015, *15*, 3711–3721.

[69] Dorrello, N. V., Peschiaroli, A., Guardavaccaro, D., Colburn, N. H. et al., S6K1- and betaTRCP-mediated degradation of PDCD4 promotes protein translation and cell growth. *Science* 2006, *314*, 467–471.

[70] Carracedo, A., Ma, L., Teruya-Feldstein, J., Rojo, F. et al., Inhibition of mTORC1 leads to MAPK pathway activation through a PI3K-dependent feedback loop in human cancer. *J. Clin. Invest.* 2008, *118*, 3065–3074.

[71] Sharma, K., Schmitt, S., Bergner, C. G., Tyanova, S. et al., Cell type- and brain region-resolved mouse brain proteome. *Nat. Neurosci.* 2015, *18*, 1819–1831.